Comparing branches of basal dendrites of human and mouse hippocampal CA1 pyramidal neurons with Bayesian networks

Bojan Mihaljević[1,*], Pedro Larrañaga[1], Ruth Benavides-Piccione[2], Javier DeFelipe[2], and Concha Bielza[1]

[1]Computational Intelligence Group, Departamento de Inteligencia Artificial, Universidad Politécnica de Madrid, Boadilla del Monte, 28660, Spain
[2]Laboratorio Cajal de Circuitos Corticales, Universidad Politécnica de Madrid and Instituto Cajal (CSIC), Pozuelo de Alarcón, 28223, Spain
[*]bmihaljevic@fi.upm.es

ABSTRACT

Pyramidal neurons are the most common cell type in the cerebral cortex. The extent to which they differ between species is a long-standing question of interest in neuroscience. A recent study analized 54 human and 50 mouse pyramidal neurons of the CA1 region of the hippocampus in order to compare the morphology of dendritic branches, primarily their length and average diameter. We extend that study with additional analyses and comparison of basal dendrites. In addition to branch length and average diameter, we consider branch tortuosity, bifurcation angles and tilt angless. To account for heterogeneity accross morphometric determinants such as branch type (whether the branch is terminal or not), branch order, and the distance from the soma, we model the branch-level morphologies with multivariate models.In particular, we learn from our data set conditional linear Gaussian Bayesian networks over the determinants and the morphologies. This lets us discover both marginal and conditional independencies among the morphometric determinants and the morphometrics as well as to assess the direction and magnitude of the probabilistic relationships among them. We report a number of novel findings. Our study illustrates a useful methodology for inter-species comparison of morphologies.

Introduction

Pyramidal neurons are the most common neuronal type in the cerebral cortex. A key challenge in neuroscience is to understand how these neurons differ across species. While an influential idea is that they can be extrapolated across species[1], a number of studies have found it rather implausible[2–5]. Since the morphology of pyramidal cells varies across layers and cortical regions within a single species[5–10] (more so in primates than in rodents[2,3]), it is important to compare neurons from homologous regions of the two species. For the human and the mouse, one such region is the hippocampus, one of the most evolutionary conserved archicortical regions[11].

A recent study[12] compared digitally reconstructed morphologies of pyramidal cells' dendrites from the hippocampus CA1 area of human and mouse. Because the dendritic trees were incompletely reconstructed, they focused on branch-level morphometrics, namely on branch length, surface, volume and average diameter. They studied how these morphometrics differed between the species, primarily by testing hypotheses of location difference via the Kruskal-Wallis test. Because the morphometrics vary, within a species, with respect to determinants such as branch type (whether a branch is terminal or not) and branch order, they further split the branches into terminal and non-terminal ones as well as according to branch order. They then ran Kruskal-Wallis tests of hypotheses of location difference between pairs of these subsets of branches, e.g., that mouse terminal branches of branch order two are as long as human terminal branches of the same branch order. They reported findings such as: (a) human dendritic branches are longer and thicker than mouse ones; (b) in both species, terminal branches are longer than non-terminal ones; and (c) in both species, branch diameter seems to decrease with increasing branch order for non-terminal branches yet stays roughly constant for the terminal ones. The authors deduced (c) by rejecting hypotheses of equal diameters across all branch orders, yet did not quantify the extent and significance of the correlation between branch order and branch diameter.

Instead of splitting the branches with respect to the morphometric determinants, one can compactly compare the morphologies with a multivariate model. For example, when naively testing whether human and mouse branches differ in length, a Kruskal-Wallis test could mislead us if there are proportionally more non-terminal branches in the human data set than in the

mouse one [1]. Namely, because non-terminal branches are shorter than terminal ones, we might not reject the null hypothesis of equal length, although we would have if we had accounted for branch type (i.e., whether terminal or non-terminal), as human non-terminal branches are longer than mouse non-terminal ones while human terminal branches are also longer than mouse terminal branches. Instead of splitting our branches according to branch type and running two tests, we could specify a multivariate statistical model over three random variables: species, branch type and branch length. Models such as Bayesian networks (BNs)[?,13,14] can represent the probabilistic relationships among the variables of a domain, while algorithms for learning Bayesian networks from data can uncover such relationships. Thus, learning a Bayesian network from our data would tell us that the species variable and the length variable are (marginally) independent yet dependent given branch type. Note that probabilistic dependence does not imply different locations (e.g., mean or median), as a morphometric could be dependent on the species variable while having the same mean and median, yet different variance, in the two species. By modelling our morphometric determinants and morphometrics as random variables, we can quantify the dependence between pairs of continuous variables with measures such as linear correlation [2] and thus, for example, formally assess whether branch diameter increases with distance from the soma. In addition, we can discover dependencies between the morphometrics themselves. An additional benefit of Bayesian networks is that they provide a compact probabilitic representation of branch-level morphology that can simplify comparison between species.

In this paper, we extend the mentioned study on hippocampus cells[12] (henceforth 'the previous study') with an analysis based on Bayesian networks. We use the same data set yet focus on basal dendrites alone and, in addition to branch length and average branch diameter, consider three additional branch-level morphometrics: tortuosity, bifurcation angles and tilt angles. We study how these morphometrics vary according to four morphometric determinants —species, branch type, branch order, and Euclidean distance from the soma— by learning from data joint Bayesian network models over the morphometrics and the determinants. We use conditional linear Gaussian Bayesian networks (CLGBNs), a particular model that assumes that the morphometrics follow a multivariate normal distribution when conditioned on a joint assignment to the discrete determinants, allowing us to jointly model both discrete and continuous variables. In addition to studying the probabilistic relationships among the variables, we also complement the previous study with Kruskal-Wallis tests of location difference regarding branch tortuosity, and bifurcation and tilt angles, that is, the morphometrics that were not covered in the previous study.

We learned Bayesian networks from three different subsets of our data set: (a) from terminal branches alone; (b) from non-terminal branches alone; and (c) from both terminal and non-terminal branches. Because terminal and non-terminal branches differ according to most morphometrics[12], separating the data into (a) and (b) lets us learn models that are specific to each branch type, whereas (c) allows us to study the effect of the branch type variable on the morphometrics. For each data subset (that is, (a), (b), and (c)), we learned a separate model for each species as well as a combined model for both species. Again, the species-specific models give us insight into the characteristics of a species whereas the combined ones let us assess the effect of the species variable on the morphometrics.

The rest of this paper is structured as follows. Section 2 describes the data set, the morphometrics, and the applied method. Section 3 provides the results. We discuss our findings in Section 4, placing them in the context of the previous study.

Methods

Data

All morphology reconstructions were obtained and analyzed in previous studies[12,15] (see Figure 1b). There were 54 human neurons, obtained from a male aged 45 and a female aged 53, obtained within a postmortem interval of 2–3 hours. There were 50 mouse neurons, obtained from nine C57BL/6 adult (8-week-old) male mice. Voxel sizes of $0.240 \times 0.240 \times 0.29\ \mu m^3$ and $0.120 \times 0.120 \times 0.13\ \mu m^3$ were used for human and mouse cells, respectively. 3D coordinates of the nodes of dendritic morphology were extracted using Neurolucida 360 (MicroBrightfield, VT, USA). Some branches were not fully included within a section and were therefore incompletely reconstructed. For further details on tissue reconstruction, intracellular injections, immunocytochemistry, and cell reconstruction, see[12].

We omitted all incomplete branches from our analysis. Figure 1b shows the counts of complete branches per species, branch type, and branching order. We only considered branches from branch order zero to branch order four. We removed 6 branches that had zero length and/or zero diameter. When these branches had descendant branches we decreased their branching order, as if the zero-length and zero-diameter branches were inexistent. We omitted from our analysis 23 branches that had a single child branch, as well as one trifurcating branch, because angles are only defined for branches that bifurcate (i.e., have exactly two child branches); we kept the descendants of these branches. Our final sample consisted of 2462 branches, 1672 from 54 human interneurons and 790 branches from 50 mouse interneurons. There were 136 ± 95 branches per each combination of species, branch type, and branching order (not considering branch order 0 for terminal branches, as there were none of this order).

[1] This is not possible in principle, as half the branches of a bifurcating tree are terminal ones and the other half are non-terminal ones. However, in practice it is: in our data set many branches were removed as they were incompletely reconstructed, altering this proportion.

[2] Note that we use the term correlation to denote both linear correlation as well as in the broader sense of probabilistic dependence.

Morphometrics

Because some branches were incompletely reconstructed, we did not use morphometrics that depend on the arbor being complete, such as total arbor length or topological variables such as partition asymmetry. Instead, we focused on five branch-level morphometrics (see Figure 1c). Namely, we computed the branch length (`length`); remote bifurcation angle (`bifurcation_angle`); remote tilt angle (`tilt_angle`); average branch diameter (`diameter`); and branch tortuosity (`tortuosity`). We considered one continuous morphometric determinant, namely, the Euclidean distance from the branch starting point to the soma (`distance`), and three discrete ones, namely: species (`species`), (centrifugal) branch order (`branch_order`), and branch type (i.e., whether terminal or non terminal; `branch_type`). Note that bifurcation angles are only defined for non-terminal branches. While the previous study analyzed branch surface and branch volume, in addition to `length` and `diameter`, we ommited these variables as they were deterministic functions of `diameter` and `length` and thus added no information not already contained in `diameter` and `length`. We computed all morphometrics and determinants with the open-source NeuroSTR library.[3]

Bayesian networks

A Bayesian network (BN)[13] $\mathscr{B}$ allows us to compactly encode a joint probability distribution over random variables $\mathbf{X}$ by exploiting conditional independencies among triplets of sets of variables in $\mathbf{X}$ (e.g., X is independent of Y given Q and Z). A BN consists of a directed acyclic graph (DAG) $\mathscr{G}$ and a set of parameters θ ($\mathscr{B} = (\mathscr{G}, \theta)$). The vertices (i.e., nodes) of $\mathscr{G}$ correspond to the variables $\mathbf{X}$ while its directed edges (i.e., arcs) encode the conditional independencies among $\mathbf{X}$. A joint probability distribution $P_{\mathscr{G}}(\mathbf{x})$ encoded by $\mathscr{B}$, where $\mathbf{x}$ is an assignment to $\mathbf{X}$, factorizes as a product of local conditional distributions,

$$P_{\mathscr{G}}(\mathbf{x}) = \prod_{i=1}^{n} P_{\mathscr{G}}(x_i \mid \mathbf{pa}_{\mathscr{G}}(x_i)),$$

where $\mathbf{pa}_{\mathscr{G}}(x_i)$ is an assignment to variables $\mathbf{Pa}_{\mathscr{G}}(X_i)$, the set of parents of X_i in $\mathscr{G}$ (for a continuous variable, the probability mass function $P_{\mathscr{G}}(X_i)$ is replaced with a density function $f_{\mathscr{G}}(X_i)$). $\mathscr{G}$ induces conditional independence constraints for $P_{\mathscr{G}}(\cdot)$, derivable from the basic constraints that each X_i is independent of its non-descendents in $\mathscr{G}$ given $\mathbf{Pa}_{\mathscr{G}}(X_i)$. For example, for any pair of variables $X \in \mathbf{X}$ and $Y \in \mathbf{X}$ that are not connected by an arc in $\mathscr{G}$ there exist a set of variables $\mathbf{Z} \subset \mathbf{X}$ ($X \notin \mathbf{Z}$, $Y \notin \mathbf{Z}$) such that X and Y are independent conditionally on $\mathbf{Z}$ (i.e., $P_{\mathscr{G}}(X, Y \mid \mathbf{Z}) = P_{\mathscr{G}}(X \mid \mathbf{Z}) P_{\mathscr{G}}(Y \mid \mathbf{Z})$). The structure $\mathscr{G}$ thus lets us identify conditional independence relationships among triplets of sets of variables: for example, no variable is independent of its parent in $\mathscr{G}$, regardless of the conditioning set $\mathbf{Z}$. These constraints extend to nodes not connected by an arc in $\mathscr{G}$ and thus, for example, in $\mathscr{G} = X \to Y \to Z$, we have that X is not marginally independent of Z but it is independent of Z conditional on Y.

The parameters θ specify the local conditional distributions (densities) $P_{\mathscr{G}}(X_i \mid \mathbf{pa}_{\mathscr{G}}(x_i))$ ($f_{\mathscr{G}}(x_i \mid \mathbf{pa}_{\mathscr{G}}(x_i))$) for each variable X_i. When $\mathbf{X}$ contains both discrete and continuous variables, as in our case, a common approach is to let $P_{\mathscr{G}}(\mathbf{x})$ be a conditional linear Gaussian distribution (CLG)[16]. The CLG only allows discrete parents in $\mathscr{G}$ for the discrete variables $\mathbf{D} \subset \mathbf{X}$ and therefore the local conditional distribution of each discrete variable $D_i \in \mathbf{D}$ is a multinomial distribution. The local conditional density $f_{\mathscr{G}}(g_i \mid \mathbf{pa}_{\mathscr{G}}(g_i))$ for a continuous variable $G_i \in \mathbf{G}$, where $\mathbf{G} = \mathbf{X} \setminus \mathbf{D}$, is

$$f_{\mathscr{G}}(g_i \mid \mathbf{pa}_{\mathscr{G}}(g_i)) = f_{\mathscr{G}}(g_i \mid \mathbf{pa}^{\mathbf{d}}_{\mathscr{G}}(g_i), \mathbf{pa}^{\mathbf{g}}_{\mathscr{G}}(g_i)) = \mathscr{N}(g_i; \beta_0^{(\mathbf{pa}^{\mathbf{d}}_{\mathscr{G}}(g_i))} + \beta^{(\mathbf{pa}^{\mathbf{d}}_{\mathscr{G}}(g_i))T} \mathbf{pa}^{\mathbf{g}}_{\mathscr{G}}(g_i), \sigma_i^{(\mathbf{pa}^{\mathbf{d}}_{\mathscr{G}}(g_i))2}),$$

where $\mathbf{pa}^{\mathbf{d}}_{\mathscr{G}}(g_i)$ is an assignment to the discrete parents of G_i and $\mathbf{pa}^{\mathbf{d}}_{\mathscr{G}}(g_i)$ an assignment to the continuous parents of G_i. There is thus a different vector of coefficients (β, σ^2) for each assignment $\mathbf{pa}^{\mathbf{d}}_{\mathscr{G}}(g_i)$ and indeed the conditional density $f(\mathbf{g} \mid \mathbf{d})$ is a multivariate normal. The $P_{\mathscr{G}}(\mathbf{x})$ is a mixture of multivariate normal distributions over $\mathbf{G}$, with one component for each instantiation $\mathbf{d}$ of $\mathbf{D}$.

Learning Bayesian networks from data

Learning $\mathscr{B}$ from a data set $\mathscr{D} = \{(\mathbf{x}^1), \ldots, (\mathbf{x}^N)\}$ of N observations of $\mathbf{X}$ involves two steps: (a) learning the DAG $\mathscr{G}$; and (b) learning θ, the parameters of the local conditional distributions. There are two main approaches to learning $\mathscr{G}$ from $\mathscr{D}$[13]: (a) by testing for conditional independence among triplets of sets of variables (the *constraint-based* approach); and (b) by searching the space of DAGs in order to optimize a score such a penalized likelihood (the *score-based* approach). While seemingly very different, conditional independence tests and network scores are related statistical criteria[17]. For example, when considering whether to include the arc $Y \to X$ into a graph $\mathscr{G}$, the likelihood-ratio test of conditional independence of X and Y given $\mathbf{Pa}_{\mathscr{G}}(X)$ and the Bayesian information criterion[18] (BIC) score are both functions of $\log \frac{\mathrm{P}(X \mid \mathbf{Pa}_{\mathscr{G}}(X), Y)}{\mathrm{P}(X \mid \mathbf{Pa}_{\mathscr{G}}(X))}$. They differ in computing the threshold for determining independence: the former relies on the distribution of the statistic under the null model (i.e.,

[3] https://computationalintelligencegroup.github.io/neurostr/

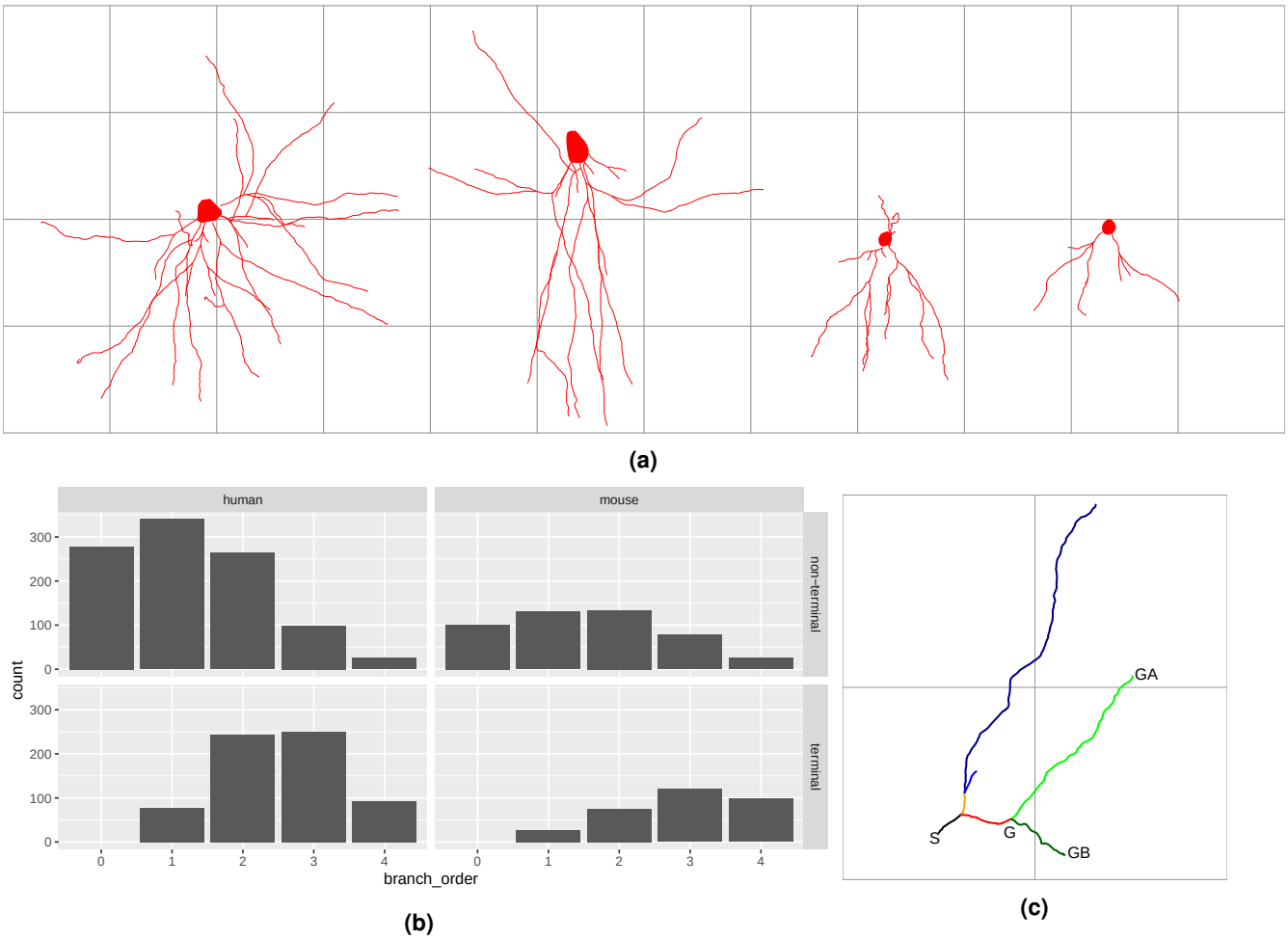

Figure 1. (a) Examples of two human (left) and mouse (right) pyramidal cells' basal dendrites. (b) Branch frequencies per branch order. We only considered branches from branch order zero to branch order four, as only 4% of the branches corresponded to higher branching orders. There were more human than mouse branches (1672 and 789, respectively) and more non-terminal than terminal branches (1475 and 986, respectively). In both species, roughly 60% of the branches were non-terminal. (c) An illustration of the computed morphometrics and morphometric determinants. A branch is a sequence of straight lines (i.e., segments) between between consecutive bifurcation points (each is branch shown with a different color in the graphic). Branch orders (variable `branch_order`) are computed centrifugally, with branch order zero corresponding to branches emanating from the soma (the black branch). The length (`length`) of a branch is the sum of the lengths of its segments. The average diameter (`diameter`) of a branch is the weighted average of the diameters of the branches' segments. Non-terminal branches (black, red and orange branches) bifurcate while terminal ones do not (binary variable `branch_type`). The Euclidean distance from the soma (`distance`) is the length of the straight line from the dendrites' insertion point into the soma up to the starting point of a branch; for the green branches, this is the distance between S and G. Note that this distance is usually computed up to the end of a branch; however, the distances in our data set are short compared to the length of terminal branches, making length a large fraction of distance and thus inducing a correlation between `distance` and `length`. `distance`, `length`, and `diameter` are all measured in micrometers (μm). `tortuosity` is the ratio of `length` and the length of the straight line between the beginning and the end of a branch; it is a unitless quantity and `tortuosity` $= 1$ denotes a perfectly straight branch whereas increasing values denote more tortuous branches. Remote bifurcation angle (`bifurcation_angle`) is the shortest planar angle between the vectors from the bifurcation to the endings of the daughter branches; for the red branch, it is the smaller angle between GA, G, and GB. Remote tilt angle (`tilt_angle`) is the smallest angle between the branch director vector and the vectors from the bifurcation to the endings of the daughter branches. `bifurcation_angle` and `tilt_angle` are measured in radians. Note that `bifurcation_angle` and `length` are undefined for terminal branches, as they do not bifurcate.

conditional independence) whereas the latter is based on an approximation to the Bayes factor between the null and alternative models. Besides using different criteria, the constraint-based and score-based approaches also differ in model search, that is, in terms of the sets X, Y, and $\mathbf{Z}$ that they choose to test conditional independence for. The score-based approaches tend to be more robust[13], as they may reconsider previous steps in the search by removing or reversing previously added arcs. A typical score-based search algorithm is hill climbing, a local search which starts from some initial DAG $\mathcal{G}$ and greedily adds, removes or reverses arcs as long as that improves the score of the DAG. While classical hypothesis testing of conditional independence might be more in line with previous work on this data set[12], score-based learning allows for more robust algorithms while still using sound statistical criteria for independence testing. We thus used the latter approach in this paper.

Location tests

We complement the previous study[12] with location tests for `tortuosity` , `bifurcation_angle`, and `tilt_angle` morphometrics that were not considered in that paper. Although t-tests and the ANOVA fit more naturally with conditional linear Gaussian Bayesian networks, we follow the previous study and apply Kruskal-Wallis rank sum tests.

Goodness-of-fit tests

We test our assumptions that the morphometrics are normally distributed conditional on `species`, `branch_type` and `branch_order` (see subsection 2.8) with the Kolmogorov-Smirnov (KS) test. Note that higher power tests, such as the Shapiro-Wilk (SW), would lead to more rejections on the Gaussian hypothesis in our data. However, we use the KS test as a loose argument that normallity is a reasonable simplifying assumption (given a non-rejection by the KS test), regardless of whether it is actually realistic, which is better tested by a test such as the SW.

Settings

As mendioned above, we consider three basic settings for learning Bayesian networks: from terminal branches alone (Section 3.2); from non-terminal branches alone (Section 3.3); and from both terminal and non-terminal branches (Section 3.4). In each setting, we learn three networks: one for the human branches; one for the mouse branches; and a combined model for branches of both species. Branching angles are only defined for non-terminal branches, and thus we omit them in models of terminal branches (Section 3.2) as well as in combined models of terminal and non-terminal branches (Section 3.4). In Section 3.4 we focus on the `branch_type` node and avoid analyzing dependencies among morphometrics, as branch-type specific dependencies can get obfuscated with the combined data from terminal and non-terminal branches that we use in Section 3.4.

All branches at branch order 0 had zero distance from the soma. To avoid a singular conditional Gaussian distribution for `distance`, we replaced these zeros by sampling from a normal distribution with mean 0 and standard deviation $1e-5$.

We learned network structures by using the tabu algorithm[19], implemented in the bnlearn[20] R[21] package, to optimize the BIC score. The tabu algorithm is a local search that efficiently allows for score-degrading operators by avoiding those that undo the effect of recently applied operators; we used a tabu list of 30 and allowed for up to 30 iterations without improving network score. We used $\alpha = 0.05$ as the significance threshold for the Kruskal-Wallis tests.

Assumptions

By using a $P_{\mathcal{G}}(\mathbf{x})$ encoded with a CLGBN to represent $P(\mathbf{x})$, we are assuming the following on $P(\mathbf{x})$: (a) the conditional independencies in $P(\mathbf{x})$ can be represented with a DAG; (b) $f(\mathbf{g} \mid \mathbf{d})$ is a multivariate normal density for each $\mathbf{d}$; and (c) that variables in $\mathbf{D}$ have no parents in $\mathbf{G}$ in the DAG of $P(\mathbf{x})$. In particular, (b) states that for each combination of `species`, `branch_type`, and `branch_order`, the distribution over `diameter`, `length`, `tortuosity` , `distance`, `bifurcation_angle`, and `tilt_angle` is a multivariate normal. This in turn means that: (i) the morphometrics marginally follow a Gaussian distribution; and (ii) the dependencies among them are linear. We consider that (ii) is reasonable modeling assumption given the number of cases (136 ± 95 branches, on average, per combination of type, and species, and branching order, see Section 2.1) whereas (i) is a common simplifying assumption. In addition, violations of (b) do necessarily lead to wrong arcs in $\mathcal{G}$, and we are precisely interested in the learning structure of $\mathcal{G}$ rather than in accurate estimation of $P(\mathbf{x})$. Since 3 of our 9 variables are discrete, (c) means that a significant number of arcs in $\mathcal{G}$ might have forced directions, as `species`, `branch_type`, and `branch_order` can have no parents in $\mathcal{G}$.

Maximizing the (penalized) likelihood of a model assumes that the data points were sampled independently from the generating distribution. Our data points are branches, with many branches coming from the same neuron and thus not necessarily independent (e.g., perhaps some cells have larger branches than others). Also, the cells come from different subjects and animals and the dendritic branches might differ among them. While violating the independence assumption might bias structure learning[22], we have, for simplicity, proceeded without checking it or accounting for it.

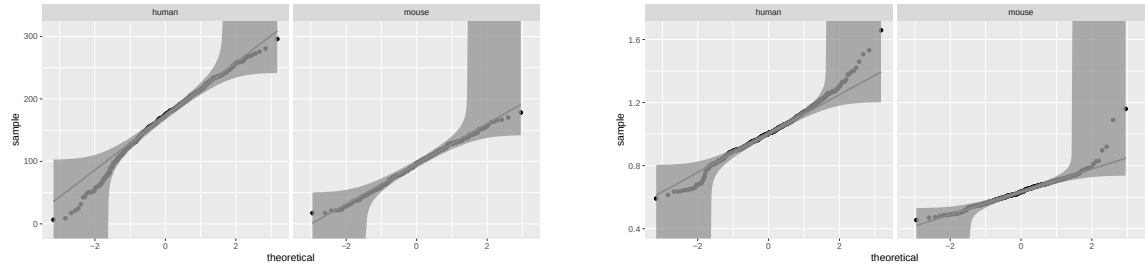

Figure 2. Q-Q plots of `length` (a) and `diameter` (b) of terminal branches. Normality is not rejected for either distribution, with the distribution of mouse `length` especially close to the theoretical one. The plots show quantiles of the sample distributions on the Y axis and the quantiles of the standard normal distribution on the X axis. For distributions that do not deviate much from normality the points lie close to the straight line. 95% Kolmogorov-Smirnov confidence bands are shown; the hypothesis of normality is rejected at the 5% level if the sample does not fall completely within the bounds.

Results

We begin by assessing whether the conditional distributions of the morphometrics can be reasonably approximated with a Gaussian distribution (Section 3.1). We then learn Bayesian networks from terminal branches (Section 3.2), non-terminal branches (Section 3.3), and both terminal branches and non-terminal branches (Section 3.4).

Morphometrics' conditional distributions

We now assess our assumption that the morphometrics are normally distributed when conditioned on `species`, `branch_type` and, optionally, `branch_order`. Considering the morphometrics' distributions conditional on species and branch type (i.e., of the form $P(X \mid \texttt{species},\texttt{branch\_type})$), the KS test did not reject normality (at the 0.05 threshold) for 6 out of 20 conditional distributions (see Table 1 in the appendix), including `bifurcation_angle` and `diameter` of terminal branches for both species, as well as `length` of mouse terminal branches (p-value 0.98, see Figure 2a). When also conditioning on branch order (i.e., considering distributions of the form $P(X \mid \texttt{species},\texttt{branch\_type},\texttt{branch\_order})$), the KS test did not reject normality for 68 out of 90 conditional distributions (see Table 2 in the appendix). This included `bifurcation_angle` and `tilt_angle` regardless of species, branch type and branch order, as well as `length` and `diameter` of terminal branches for either species (see Figure 2b). On the other hand, normality was rejected at most branch orders for the `length` of non-terminal branches and `tortuosity` of human branches. In summary, after accounting for `branch_order`, we find that the conditional distributions of most morphometrics can be approximated with Gaussian distributions.

Terminal branches

The human and mouse BNs (Figure 3a and Figure 3b, respectively) only differed in that the `tortuosity` $\rightarrow$ `distance` arc was present in the mouse BN yet not in the human one.

In both networks, `branch_order` was (marginally) correlated with `distance` and `length` yet not with `diameter` and `tortuosity`. `distance`, naturally, increased with `branch_order` (in both species; Figure 4). For both species, `length` decreased with `distance` (see Figure 3d), somewhat more sharply for the mouse than for the human (-0.58 correlation between `length` and `distance` for the mouse and -0.41 for the human), and indeed was independent of `branch_order` given `distance`.

For both species, branch `diameter` was independent of all variables, including `branch_order` and `length`, as the `diameter` node was disconnected from the rest of the graph in Figure 3a and Figure 3b. `tortuosity` and `length` were marginally independent in the mouse BN; while the human BN does not imply independence (there is a path `tortuosity` $\rightarrow$ `distance` $\rightarrow$ `length`), the marginal correlation of `tortuosity` and `length` was actually not significant[4]. This is, perhaps, surprising, as one might expect longer branches to be more tortuous.

The combined BN for terminal branches (Figure 3c) shows that the distributions of all morphometrics differed between species, even after accounting for `branch_order`, since there were arcs from the `species` node to all morphometrics. As reported by the previous study, human terminal branches were thicker and longer. We also found that they were less tortuous than

[4]We found that no arc was added when learning a Bayesian network over `tortuosity` and `length` nodes alone. Also, a test of marginal linear correlation returned a p-value of 0.11.

mouse terminal branches (Figure 4). While species and distance were marginally independent[5] (Figure 4), the species → distance arc in Figure 3c) indicates that distance differs between species once we account for branch_order: namely, human branches are further away from the soma than mouse branches of the same branching order (Figure 4). This dependence between species and distance is marginally obfuscated because there are proportionally more higher order terminal branches in the mouse data set than in the human one (see Figure 1b).

Non-terminal branches

Unlike for terminal branches, there were a number of differences between the human (Figure 5a) and mouse (Figure 5b) BNs. There are also notably more arcs (dependencies) per node among the morphometrics than for the terminal branches.

branch_order and distance were (marginally) not independent of any morhpometric in either network. In particular, length increased with distance while diameter, bifurcation_angle, and tilt_angle decreased (Figure 6a to Figure 6d). Although implied by both networks, the marginal correlation of distance with tortuosity was, however, not significant[6]. Interestingly, in the mouse network, all morphometrics were independent of branch_order and distance given diameter.

After accounting for branch_order, distance was only correlated with bifurcation_angle and tilt_angle in the human BN. Indeed, knowing distance and length renders bifurcation_angle and tilt_angle independent of branch_order in the human BN. Thus, while in terminal branches branch_order was redundant given distance, in non-terminal branches it was only redundant for bifurcation_angle and tilt_angle, only in the human BN.

As reported in the previous study, diameter decreased while length increased with branch_order and the two were (marginally) negatively correlated (see Figure 5d). After accounting for diameter, the branch_order variable added no information on length in the mouse BN while it did in the human, and hence there was no branch_order → length in the mouse BN. tortuosity was correlated with length in both species, with longer branches somewhat more tortuous on average (Figure 6e).

In both species, bifurcation_angle increased with diameter and decreased with length; in the human BN, bifurcation_angle was independent of diameter given length. tilt_angle was positively correlated with bifurcation_angle ($\rho = 0.58$ and $\rho = 0.53$ for the human and mouse, respectively) in both species. For the human, tilt_angle was independent of all other variables, including branch_order, given bifurcation_angle.

The combined BN for non-terminal branches (Figure 5c) shows that the distributions of all morphometrics differed between species. Namely, the species node was not marginally independent of any morphometric, while there were arcs from the species node to all morphometrics but tilt_angle and tortuosity . Thus, tilt_angle was independent of species given bifurcation_angle, while tortuosity was independent of species given length, diameter, and distance. As reported by the previous study, human non-terminal branches were thicker and longer than those of mouse. We found that they were less tortuous and had larger bifurcation and tilt angles (Figure 6f to Figure 6h). As in terminal branches, species and distance were marginally independent[7] (Figure 6i) yet not independent conditional on branch_order, as human non-terminal branches were located further away from the soma than mouse non-terminal branches of the same branching order (Figure 6j).

The p-values for tortuosity and distance reported in Figure 6 were orders of magnitude larger those reported in Figure 4, suggesting that the differences between species were more pronounced in terminal than in non-terminal branches. Note that there was also a large difference in p-values for length (p-values 3.550249e-93 and 1.79264e-07 for terminal and non-terminal branches, respectively) yet not for diameter (p-values 2.3895e-132 and 6.408687e-136).

All branches

All morphometrics varied with respect to species, even after accounting for branch_type and branch_order, as there was an arc from species to each morphometric in Figure 7c. While the previous study already reported such inter-species differences regarding length and diameter, Figure 7c confirms that the differences still hold after accounting for branch_type and branch_order. The lower tortuosity of human branches (Figure 4 and Figure 6) could not be fully explained by the fact that human branches are longer, as tortuosity is not independent of species given length in Figure 7c.

[5] We found that no arc was added when learning a Bayesian network over species and distance nodes alone. Also, a test Kruskal-Wallis test returned a p-value of 0.2498.

[6] We found that no arc was added when learning a Bayesian network over distance and tortuosity nodes alone. Also, tests of marginal linear correlation returned p-values of 0.13 and 0.14 for the human and the mouse, respectively.

[7] We found that no arc was added when learning a Bayesian network over species and distance nodes alone. Also, a test Kruskal-Wallis test returned a p-value of 0.1313.

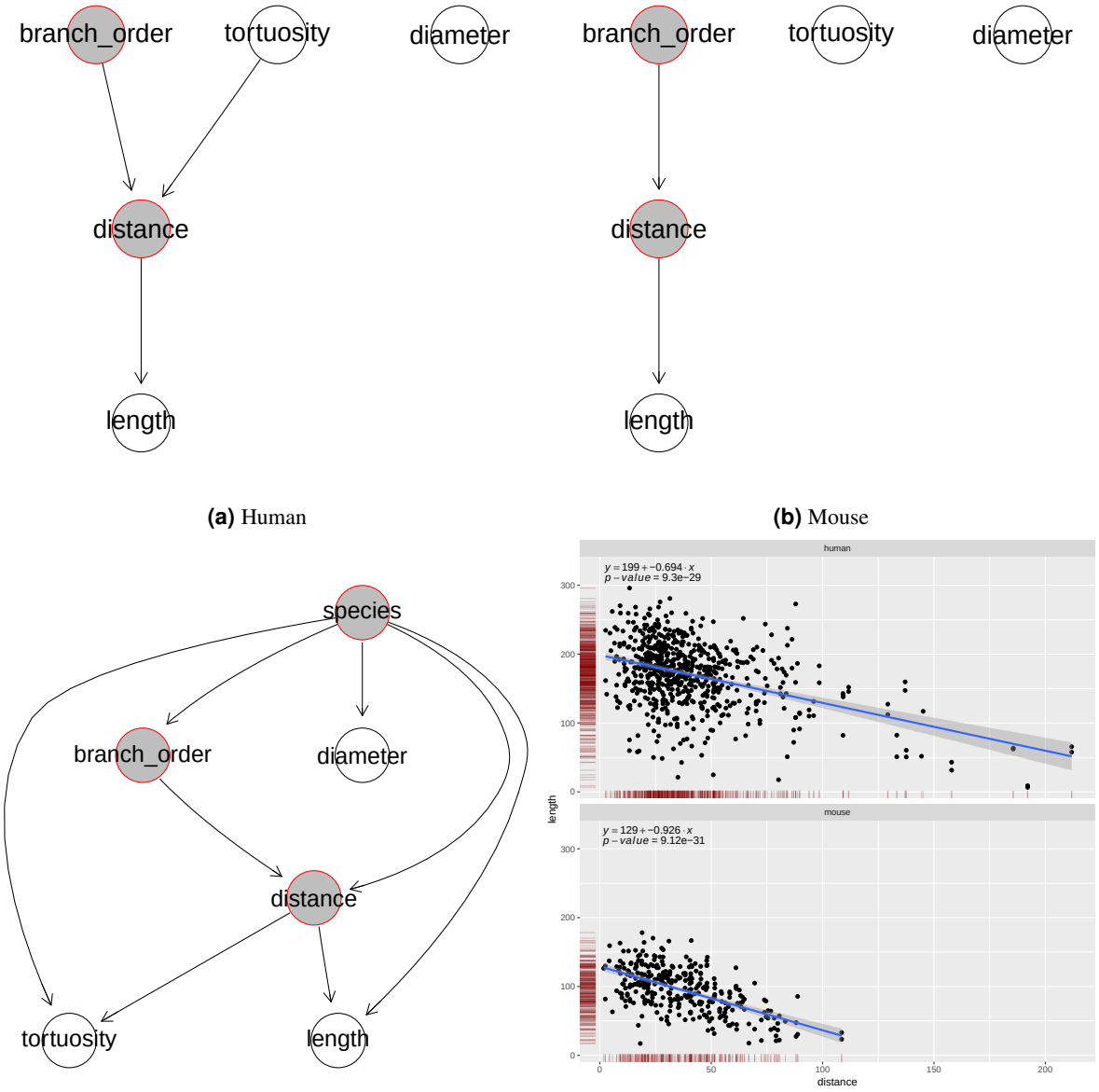

(a) Human

(b) Mouse

(c) Combined

(d) Conditional distributions of `length` for the two species

Figure 3. Bayesian networks for the terminal branches. (a) The network learned from human data alone. (b) The network learned from mouse data alone. (c) The network learned from data of both species. The nodes of the morphometric determinants are shaded in grey, with red borders. Arcs among morphometrics are depicted in red. (d) Scatter plots depicting the conditional distribution of `length` on `distance`, for the human (above) and for the mouse (below). The linear regression line shows the mean of the fitted conditional distribution of `length` given `distance`, with a 95% confidence interval.

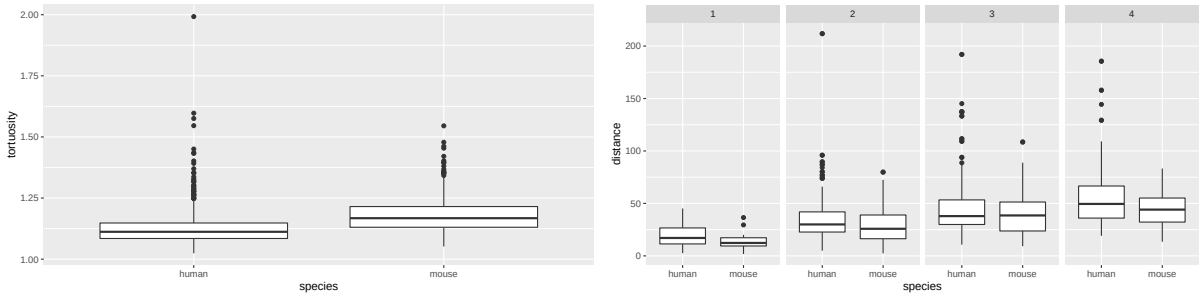

Figure 4. Terminal branches. Boxplots of the distributions of `tortuosity` and `distance` for terminal branches with respect to `species`. Since `distance` was not independent of `branch_order` in either Bayesian network, we are also showing `branch_order` in the right plot. Human terminal branches were less tortuous than mouse terminal branches (Kruskal-Wallis p-value 1.254863e-39 for `tortuosity`). Marginally, they were not located further away from the soma than mouse ones (p-value 0.2498 for `distance`) yet, for branch orders 1, 2 and 4, they were (p-values 0.009648, 0.009102, 0.07976, and 0.03981 for `distance` at branch orders 1, 2, 3, and 4, respectively).

As reported in the previous study, terminal branches were thinner and longer than non-terminal ones in both species (see also Figure 8a). We also found that, in both species, terminal branches were less tortuous and initiated further away from the soma than non-terminal ones, and that the differences, for all morphometrics, were more pronounced in human cells (see Figure 8b). The ratio between mean `length`, `diameter`, `tortuosity` and `distance` between terminal and non-terminal branches was similar across species (Figure 8b).

The fact that non-terminal are more tortuous than terminal ones cannot be completely explained by the fact that non-terminal branches are shorter, as `tortuosity` is not independent of `branch_type` given `length` in any of the networks (Figure 7c, Figure 7a, and Figure 7b). Indeed, there was an arc from `branch_type` to each morphometric, in the combined network (Figure 7c) as well as in the per-species networks (Figure 7a and Figure 7b), meaning that differences between terminal and non-terminal branches could not be fully explained in terms of `branch_order` and the remaining morphometrics. These seem to be, instead, intrinsic differences between terminal and non-terminal branches.

Discussion

Comparing terminal and non-terminal branches

The networks for terminal (Section 3.2) and non-terminal (Section 3.3) branches differed in terms of correlations among the variables and these differences were consistent between species. First, there were less correlations among morphometrics in terminal than in non-terminal branches, as evidenced by the fewer arcs per node in the Bayesian networks for the former. In particular, in non-terminal branches, longer branches were thinner and more tortuous than short ones, while such correlations were absent in terminal branches. Second, the conditional distributions of length and diameter of terminal branches were well approximated by a normal distribution for any branching order (see Table 2 in the appendix) yet for relatively few branching orders in the non-terminal ones. The above might suggest that there are fewer constraints on the growth of terminal branches, leading to little interaction among branch length, diameter and tortuosity.

The only shared dependences among the networks for terminal and non-terminal branches of both species (i.e., Figure 3a, Figure 3b, Figure 5a and Figure 5b) were those of `distance` and `branch_order` affecting `length`. The direction of the effect differed, however, as the branch length decreased with distance from the soma for terminal branches (Figure 3d) whereas it slighly decreased for non-terminal branches (Figure 6a).

In terminal branches, the `distance` from soma seems to be a more useful variable than `branch_order`, as `length` is independent of `branch_order` given `distance` in both the species (Figure 3a and Figure 3b) whereas in non-terminal branches `distance` alone does not render `branch_order` independent of any morphometric in either network (Figure 5a and Figure 5b). A possible explanation is the wide range of distances within a branch order for terminal branches (up to 211.81 μm in Figure 4), relative to the narrow range of distances for non-terminal branches (up to 66.93 μm in Figure 6j). Thus, when analysing terminal branches it is informative to consider the distance from the soma as complementary information to branch order whereas for non-terminal branches considering branch order alone may suffice.

The inter-species differences in the magnitude of `length` and `tortuosity` were more pronounced in terminal branches than in non-terminal ones, as suggested by the p-values of the Kruskal-Wallis tests (Section 3.3). Indeed, a similar result was observed by Deitcher and colleagues[10] regarding the branch length of basal trees of temporal cortex pyramidal neurons of the

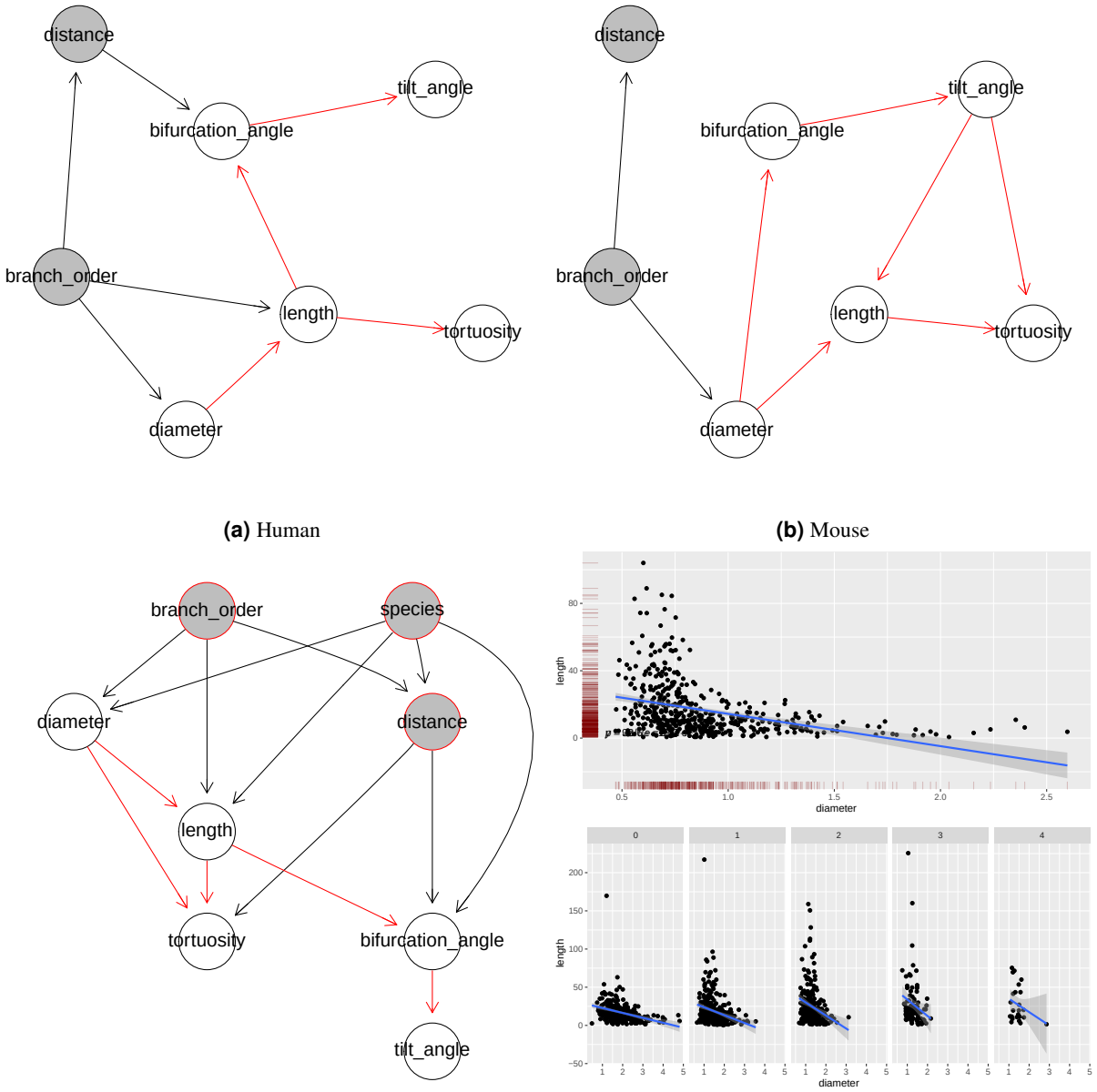

(a) Human

(b) Mouse

(c) Combined

(d) Conditional distributions of `length` for the two species

Figure 5. Bayesian networks for non-terminal branches. (a) The network learned from human data alone. (b) The network learned from mouse data alone. (c) The network learned from data of both species. The nodes of the morphometric determinants are shaded in grey, with red borders. Arcs among morphometrics are depicted in red. (d) Scatter plots depicting the conditional distribution of `length` on `diameter`, for the mouse (above), and on `diameter` and `branch_order` for the human (below). The linear regression line shows the mean of the fitted conditional distribution of `length` given `diameter`, with a 95% confidence interval; for the human there is one regression line for each value of `branch_order`.

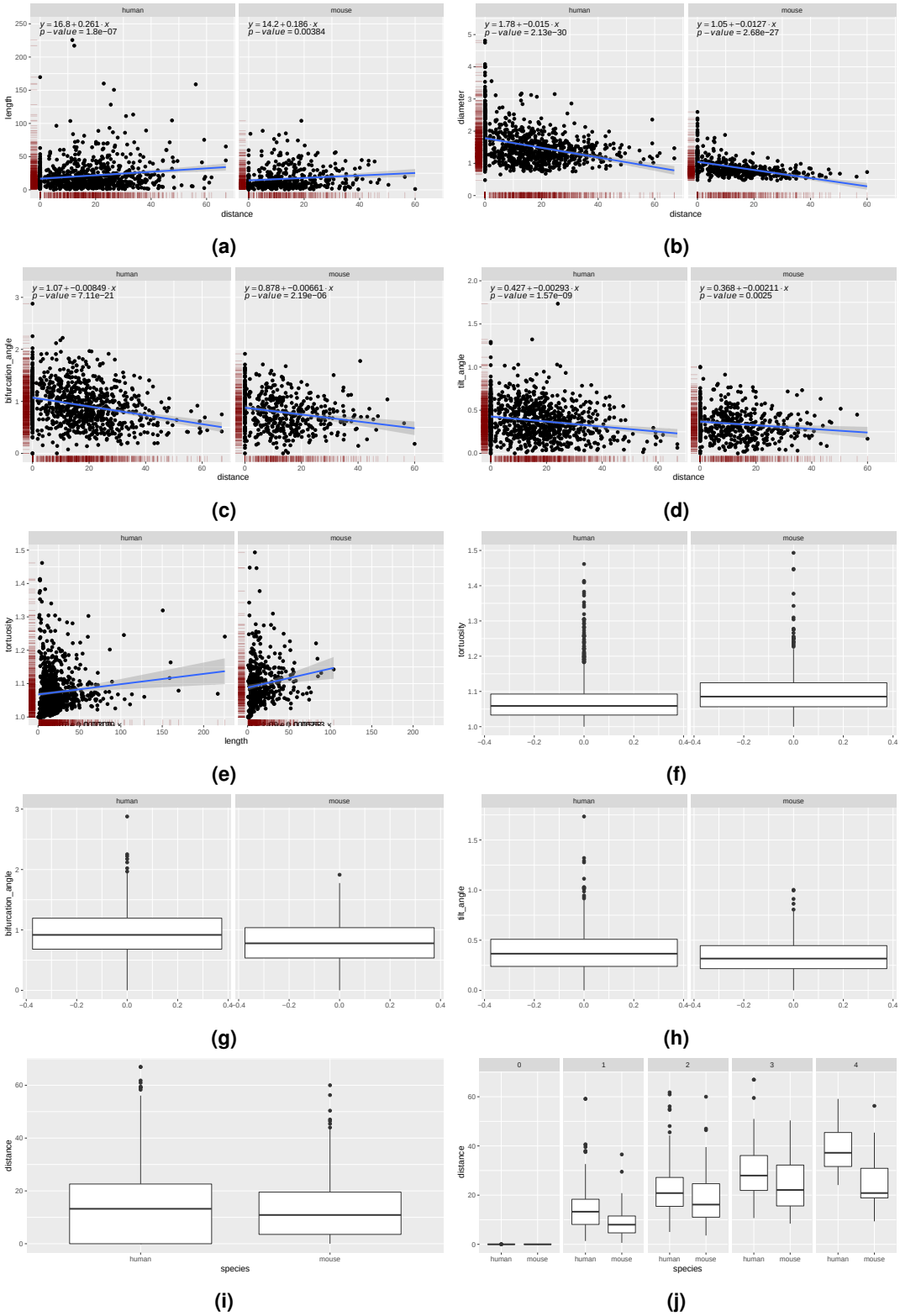

Figure 6. Non-terminal branches. (a) – (d) linear correlation of `distance` and `length`, `diameter`, `bifurcation_angle`, and `tilt_angle`, respectively. The sign of the correlation coefficient was the same for both species in all cases, with the regression lines roughly parallel. `tortuosity` as a function of `length`. (f) – (h) Human non-terminal branches were less tortuous (f), had larger bifurcating (g) and tilt angles (h). (Kruskal-Wallis p-values of 2.4899e-19, 6.840901e-13, and 0.0001 for `tortuosity` , `bifurcation_angle`, and `tilt_angle`, respectively). (i) and (j) Marginally, human non-terminal branches were not located further away from the soma than mouse ones (p-value 0.2266677 for `distance`) yet, for all branch orders except for 0, they were (p-values 0.3377, 2.397e-10, 1.814e-05, 0.0002662, and 3.386e-05 for `distance` at branch orders 0, 1, 2, 3, and 4, respectively).

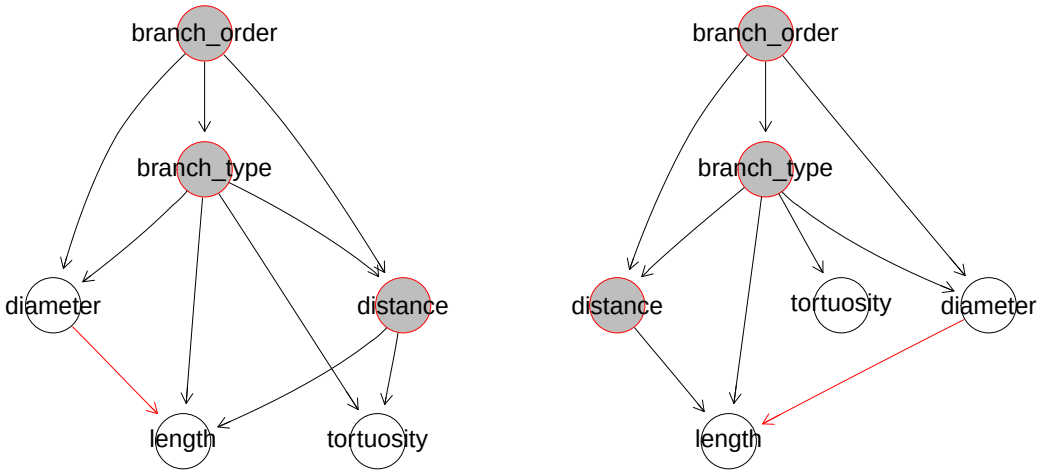

(a) Human

(b) Mouse

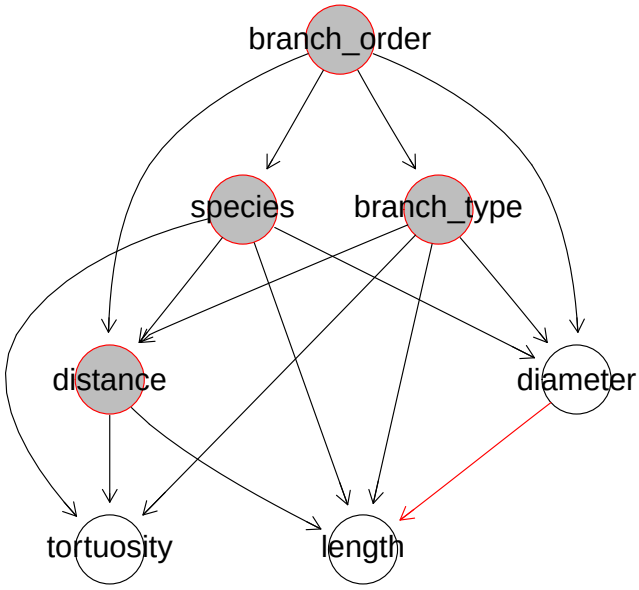

(c) Combined

Figure 7. Bayesian networks learned from all branches (terminal and non-terminal branches combined). (a) The network learned from human data alone. (b) The network learned from mouse data alone. (c) The network learned from data of both species. The nodes of the morphometric determinants are shaded in grey, with red borders. Arcs among morphometrics are depicted in red.

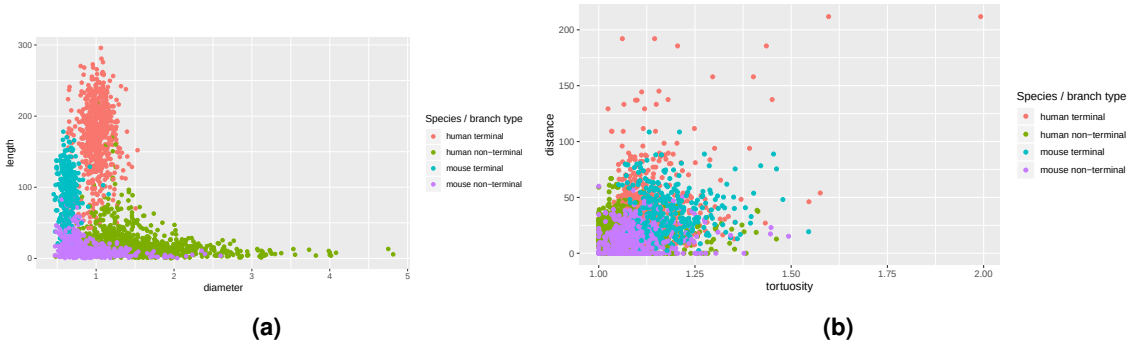

(a) (b)

Figure 8. Scatter plots of `length`, `diameter`, `tortuosity` and `distance` with respect to `species` and `branch_order`. (a) Terminal branches were longer and thinner than non-terminal ones in both species. (Kruskal-Wallis p-values of 1.100032e-253 and 1.883281e-143 for `length` and `diameter`, respectively, in the human; 5.543581e-117 and 1.882175e-55 in the mouse.) (b) Terminal branches were less tortuous and initiated further away from the soma than non-terminal ones in both species. (Kruskal-Wallis p-values of 5.816486e-92 and 3.120528e-135 for `tortuosity` and `distance`, respectively, in the human; 1.327429e-60 and 4.279025e-66 in the mouse.) Mean `length` in terminal branches was 8.289185 times the mean `length` in non-terminal branches for the human (5.689702 for the mouse); mean `diameter` was 0.6438295 times the mean `diameter` in non-terminal branches for the human (0.7220158 for the mouse); mean `tortuosity` was 1.050688 times the mean of `tortuosity` in non-terminal branches for the human (1.078793 times for the mouse); mean `distance` was 2.858884 times the mean of `distance` in non-terminal branches for the human (2.857891 for the mouse).

human and the mouse. Nonetheless, the Bayesian networks of terminal branches were similar between the species whereas those for the non-terminal branches

Correlation among morphometrics

Integestingly, `bifurcation_angle` and `tilt_angle` were negatively correlated with `length`, the length of the parent branch in a biffurcation (see Figure 5a and Figure 5b; correlation coefficients not shown). Also, in terminals branches `length` was independent of `length`, although we might expect longer branches to be more tortuos (this is indeed the case in non-terminal branches).

Bayesian networks for inter-species comparison

This study introduces Bayesian networks as multivariate models for comparison between species. We consider that multivariate models are useful for inter-species comparison because we need to account for heterogeneity that is due to morphometric determinants such as branch order and branch type, as opposed to the heterogeneity between species. Comparison by learning Bayesian networks from data, in particular, uncovers a compact representation of the branch-level morphology in terms of probabilistic relationships among both morphometrics and determinants. We find that the graphical representation of the probabilistic dependencies in the morphology of each species gives a concise representation of differences and similarities between species. In addition to network structure, the signs and magnitudes of the regression coefficients in the local distributions indicate the direction and magnitude of the probabilistic relationships. Provided that our assumptions hold (see Section 2.8), the networks we have laerned from data are faithfull models of the branch-level morphologies for the two species. As such, they could be used for more purposes that comparison; for example, to generate synthetic branches (see[23]) or perform probabilistic queries about the morphology.

References

1. Douglas, R. J. & Martin, K. A. Neuronal circuits of the neocortex. *Annu. Rev. Neurosci.* **27**, 419–451 (2004).
2. Luebke, J. I. Pyramidal neurons are not generalizable building blocks of cortical networks. *Front. Neuroanat.* **11**, 11 (2017).
3. Gilman, J. P., Medalla, M. & Luebke, J. I. Area-specific features of pyramidal neurons – a comparative study in mouse and rhesus monkey. *Cereb. Cortex* **27**, 2078–2094 (2017).
4. Elston, G. N., Benavides-Piccione, R. & DeFelipe, J. The pyramidal cell in cognition: a comparative study in human and monkey. *J. Neurosci.* **21**, RC163–RC163 (2001).

5. Mohan, H. *et al.* Dendritic and axonal architecture of individual pyramidal neurons across layers of adult human neocortex. *Cereb. Cortex* **25**, 4839–4853, DOI: 10.1093/cercor/bhv188 (2015).
6. Benavides-Piccione, R., Ballesteros-Yáñez, I., DeFelipe, J. & Yuste, R. Cortical area and species differences in dendritic spine morphology. *J. Neurocytol.* **31**, 337–346 (2002).
7. Benavides-Piccione, R., Hamzei-Sichani, F., Ballesteros-Yáñez, I., DeFelipe, J. & Yuste, R. Dendritic size of pyramidal neurons differs among mouse cortical regions. *Cereb. Cortex* **16**, 990–1001 (2006).
8. Ballesteros-Yáñez, I., Benavides-Piccione, R., Bourgeois, J., Changeux, J. & DeFelipe, J. Alterations of cortical pyramidal neurons in mice lacking high-affinity nicotinic receptors. *Proc. Natl. Acad. Sci. United States Am.* **107**, 11567–11572 (2010).
9. Rojo, C. *et al.* Laminar differences in dendritic structure of pyramidal neurons in the juvenile rat somatosensory cortex. *Cereb. Cortex* **26**, 2811–2822 (2016).
10. Deitcher, Y. *et al.* Comprehensive morpho-electrotonic analysis shows 2 distinct classes of l2 and l3 pyramidal neurons in human temporal cortex. *Cereb. Cortex* **27**, 5398–5414, DOI: 10.1093/cercor/bhx226 (2017).
11. Stephan, H. & OJ, A. *The allocortex in primates*, vol. The primate brain (Appleton Century Crofts, New York, 1970).
12. Benavides-Piccione, R. *et al.* Differential Structure of Hippocampal CA1 Pyramidal Neurons in the Human and Mouse. *Cereb. Cortex* DOI: 10.1093/cercor/bhz122 (2019). http://oup.prod.sis.lan/cercor/advance-article-pdf/doi/10.1093/cercor/bhz122/28905613/bhz122.pdf.
13. Koller, D. & Friedman, N. *Probabilistic Graphical Models: Principles and Techniques* (MIT press, Cambridge, MA, USA, 2009).
14. Bielza, C. & Larrañaga, P. Bayesian networks in neuroscience: A survey. *Front. Comput. Neurosci.* **8**, 131 (2014).
15. Domínguez-Álvaro, M. *et al.* Three-dimensional analysis of synapses in the transentorhinal cortex of Alzheimer's disease patients. *Acta Neuropathol. Commun.* **6**, 20 (2018).
16. Lauritzen, S. & Wermuth, N. Graphical models for associations between variables, some of which are qualitative and some quantitative. *The Annals Stat.* **17**, 31–57 (1989).
17. Scutari, M., Graafland, C. E. & Gutiérrez, J. M. Who learns better Bayesian network structures: Accuracy and speed of structure learning algorithms. *Int. J. Approx. Reason.* **115**, 235–253 (2019).
18. Schwarz, G. Estimating the dimension of a model. *The Annals Stat.* **6**, 461–464 (1978).
19. Glover, F. & Laguna, M. Tabu Search*. In Pardalos, P. M., Du, D.-Z. & Graham, R. L. (eds.) *Handbook of Combinatorial Optimization*, 3261–3362 (Springer, New York, NY, 2013).
20. Scutari, M. Learning Bayesian networks with the `bnlearn` `R` package. *J. Stat. Softw.* **35**, 1–22 (2010).
21. R Core Team. *R: A Language and Environment for Statistical Computing*. R Foundation for Statistical Computing, Vienna, Austria (2015).
22. Bae, H. *et al.* Learning Bayesian networks from correlated data. *Sci. reports* **6**, 1–14 (2016).
23. López-Cruz, P. L., Bielza, C., Larrañaga, P., Benavides-Piccione, R. & DeFelipe, J. Models and simulation of 3D neuronal dendritic trees using Bayesian networks. *Neuroinformatics* **9**, 347–369 (2011).

Acknowledgements

This work has been partially supported by the Spanish Ministry of Economy and Competitiveness through the TIN2016-79684-P project. This project has received funding from the European Union's Horizon 2020 Framework Programme for Research and Innovation under the Specific Grant Agreement No. 785907 (Human Brain Project SGA2).

Author contributions statement

B.M. designed and conducted the analysis and wrote the manuscript. ... All authors reviewed the manuscript.

Additional information

Branch type	Species	Tortuosity	Diameter	Distance	Length	RBA	RTA
non-terminal	human	0.00	0.00	0.00	0.00	0.16	0.03
non-terminal	mouse	0.00	0.00	0.00	0.00	0.53	0.08
terminal	human	0.00	0.08	0.00	0.04		
terminal	mouse	0.00	0.32	0.03	0.92		

Table 1. P-values for the Kolmogorov-Smirnov test of normality. Columns 1-2 indicate the groups and columns 4-9 show the p-values. BO = branch order. RBA = bifurcation angle. RTA = tilt angle. Missing entries indicate that there were no observations for a given group.

Branch type	Species	BO	Tortuosity	Diameter	Distance	Length	RBA	RTA
non-terminal	human	0	0.00	0.00		0.00	0.25	0.35
non-terminal	human	1	0.00	0.01	0.06	0.00	0.30	0.15
non-terminal	human	2	0.00	0.07	0.26	0.00	0.31	0.51
non-terminal	human	3	0.00	0.25	0.57	0.00	0.33	0.14
non-terminal	human	4	0.51	0.29	0.88	0.16	0.60	0.76
non-terminal	mouse	0	0.20	0.12		0.01	0.77	0.77
non-terminal	mouse	1	0.48	0.02	0.09	0.00	0.60	0.29
non-terminal	mouse	2	0.05	0.19	0.01	0.00	0.59	0.82
non-terminal	mouse	3	0.04	0.14	0.36	0.04	0.94	0.75
non-terminal	mouse	4	0.29	0.13	0.45	0.40	0.66	0.99
terminal	human	1	0.08	0.36	0.25	0.56		
terminal	human	2	0.00	0.28	0.00	0.31		
terminal	human	3	0.00	0.30	0.00	0.40		
terminal	human	4	0.00	0.83	0.00	0.58		
terminal	mouse	1	0.09	0.76	0.52	0.42		
terminal	mouse	2	0.71	0.20	0.08	0.85		
terminal	mouse	3	0.11	0.64	0.14	0.86		
terminal	mouse	4	0.04	0.36	0.79	0.95		

Table 2. P-values for the Kolmogorov-Smirnov test of normality. Columns 1-3 indicate the groups and columns 3-8 show the p-values. BO = branch order. RBA = bifurcation angle. RTA = tilt angle. Missing entries indicate that there were no observations for a given group.